The effect of drive frequency and set point amplitude on tapping forces in atomic force microscopy: simulation and experiment

2009 Nanotechnology 20 245703

(http://iopscience.iop.org/0957-4484/20/24/245703)

Nanotechnology **20** (2009) 245703 (10pp) doi:10.1088/0957-4484/20/24/245703

The effect of drive frequency and set point amplitude on tapping forces in atomic force microscopy: simulation and experiment

Justin Legleiter

The C Eugene Bennett Department of Chemistry, West Virginia University, 217 Clark Hall, PO Box 6045, Morgantown, WV 26506, USA

E-mail: justin.legleiter@mail.wvu.edu

Received 16 March 2009, in final form 22 April 2009
Published 27 May 2009
Online at stacks.iop.org/Nano/20/245703

Abstract

In tapping mode atomic force microscopy (AFM), a sharp probe tip attached to an oscillating cantilever is allowed to intermittently strike a surface. By raster scanning the probe while monitoring the oscillation amplitude of the cantilever via a feedback loop, topographical maps of surfaces with nanoscale resolution can be acquired. While numerous studies have employed numerical simulations to elucidate the time-resolved tapping force between the probe tip and surface, until recent technique developments, specific read-outs from such models could not be experimentally verified. In this study, we explore, via numerical simulation, the impact of imaging parameters, i.e. set point ratio and drive frequency as a function of resonance, on time-varying tip–sample force interactions, which are directly compared to reconstructed tapping forces from real AFM experiments. As the AFM model contains a feedback loop allowing for the simulation of the entire scanning process, we further explore the impact that various tip–sample force have on the entire imaging process.

1. Introduction

Since its invention in 1986 [1], the atomic force microscope (AFM) has become a standard technique in imaging structure and measuring physical phenomena at the nanoscale. In AFM, the force interaction between a sharp probe tip affixed to a flexible cantilever and surface is measured. A laser is reflected off the back of the cantilever and focused onto a position-sensitive photodetector, creating an optical lever capable of measuring the vertical deflection of the cantilever with sub-angstrom resolution. Images are formed by raster scanning the tip across the surface while using a feedback loop to monitor the force interactions between the tip and surface. Owing to its ability to significantly minimize lateral forces associated with scanning, tapping (or intermittent contact) mode AFM has become an increasingly important experimental technique in studying soft, easily damaged, nanoscale structures [2]. During tapping mode operation, the cantilever is oscillated near its resonance frequency, ω_o, resulting in a 'free' amplitude, A_o. When the cantilever is placed in close proximity to the surface, the tip intermittently contacts (or taps) the surface, resulting in a decreased cantilever oscillation amplitude from the 'free' amplitude to a 'tapping' amplitude A. The image is acquired during raster scanning over the sample by measuring the necessary adjustments to the vertical displacement of the scanner, via a feedback loop, to maintain the constant value of set point ratio $s = A/A_o$. The feedback loop provides precise control over the cantilever amplitude, and thus, the tapping force between the tip and surface.

In an effort to more fully understand the interaction between the probe tip and sample surface in tapping mode AFM, cantilever-based numerical simulations are often employed [2–10]. These simulations have been extensively used to understand the effect of various parameters on tip–sample interactions, such as the time-varying tapping forces, phase, and amplitude. Due to experimental limitations, i.e. the inability to measure time-varying tapping forces, many of the insights gained from such models have not been directly

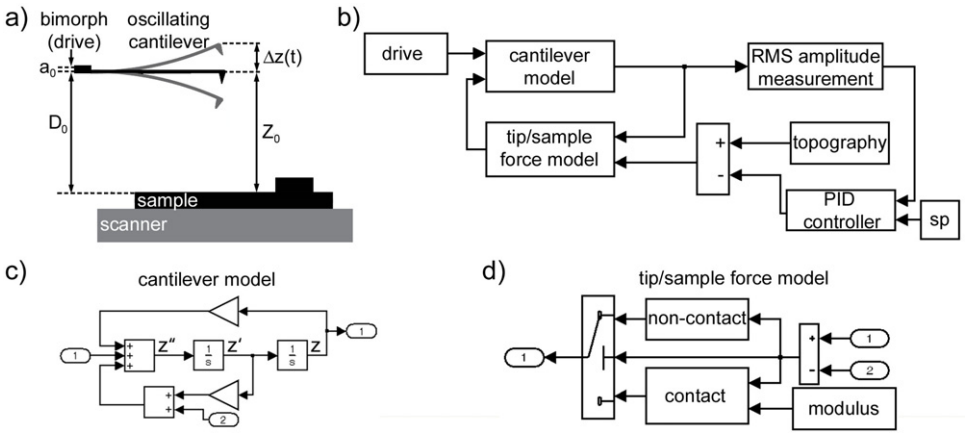

Figure 1. (a) Schematic illustration of a tapping mode AFM experimental set-up illustrating several parameters contained in equation (1) which were used to model cantilever dynamics. (b) Numerical simulations were performed with SIMULINK as illustrated. Key components of the model include the cantilever drive, cantilever model (shown in further detail in (c)), the tip/sample force model which contains the ability to change the surface modulus (shown in further detail in (d)), the amplitude measurement, the topography model, feedback loop with an PID controller, and the set point parameter (abbreviated sp).

verified experimentally. Furthermore, in most numerical simulations of tapping mode AFM, only the dynamic behavior of the cantilever has been studied, and only a relatively few studies have taken into account the transient effects observed while scanning [7, 10, 11]. One of these studies demonstrated, with experimental verification, that operating far below the resonance frequency of the cantilever can lead to greater cantilever stability, resulting in the ability to employ higher feedback gains, better feature tracking, and faster scanning rates [7]. Numerical simulations indicated that the trade-off for this increased cantilever stability was larger tip–sample forces the further below resonance the cantilever was driven; however, due to the previously mentioned limitations, this result was not experimentally verified.

Recent AFM technique development efforts have been focused on simultaneously obtaining measurements of physical properties of surfaces while imaging via tapping mode [11–17]. One method to accomplish this goal is to reconstruct the time-resolved force interaction between the tip and surface during tapping mode operation. The time-resolved tip–sample force during tapping contains information analogous to that obtained from the standard force curve experiment. The reconstruction of tapping forces has been achieved in both operation in air [12–16] and fluid [11, 18]. While the main thrust of these efforts was to extract quantitative measurements of material properties while simultaneously imaging a surface in the tapping mode, this ability now also allows for the direct comparison of time-varying tapping forces measured from experiment with numerical simulations of tapping mode AFM.

In this study, we investigate, via numerical simulation and experiment, the relationship between imaging parameters and the time-varying tapping force on both hard and soft surfaces. We first explore the influence of amplitude set point on time-varying tapping forces. Second, we determine the role drive frequency as a function of resonance plays in tip/surface force interactions. Finally, we demonstrate how the generated tapping forces influence the image of a soft nanoscale feature on hard surfaces and propose a method for estimating the true height of soft compressible features in tapping mode AFM images.

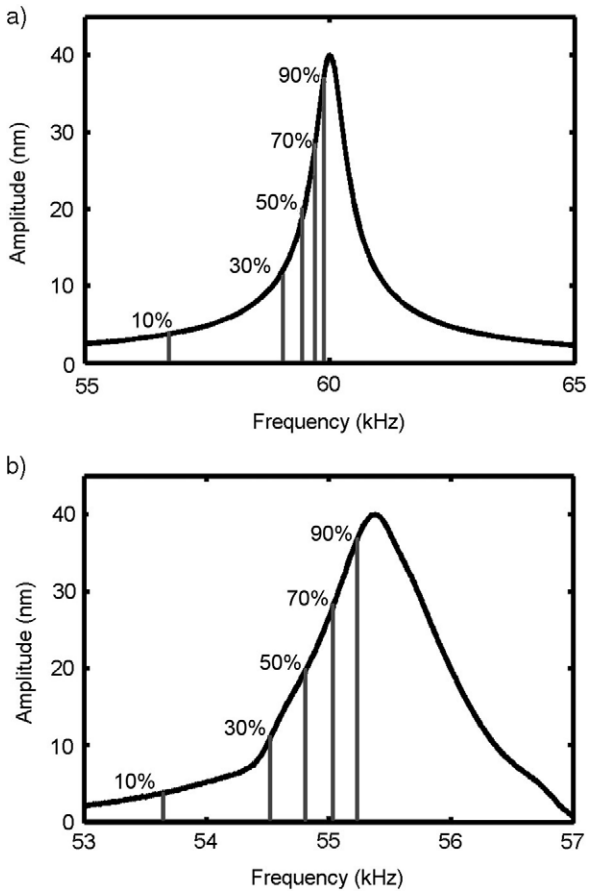

Figure 2. The amplitude response of a cantilever around its resonance frequency for both (a) simulations and (b) real experiments. Drive frequencies at specific 'x% below resonance' are indicated. x% below resonance is defined as the frequency at which the free amplitude drops down to x% of the free amplitude at the resonance frequency for any given drive amplitude.

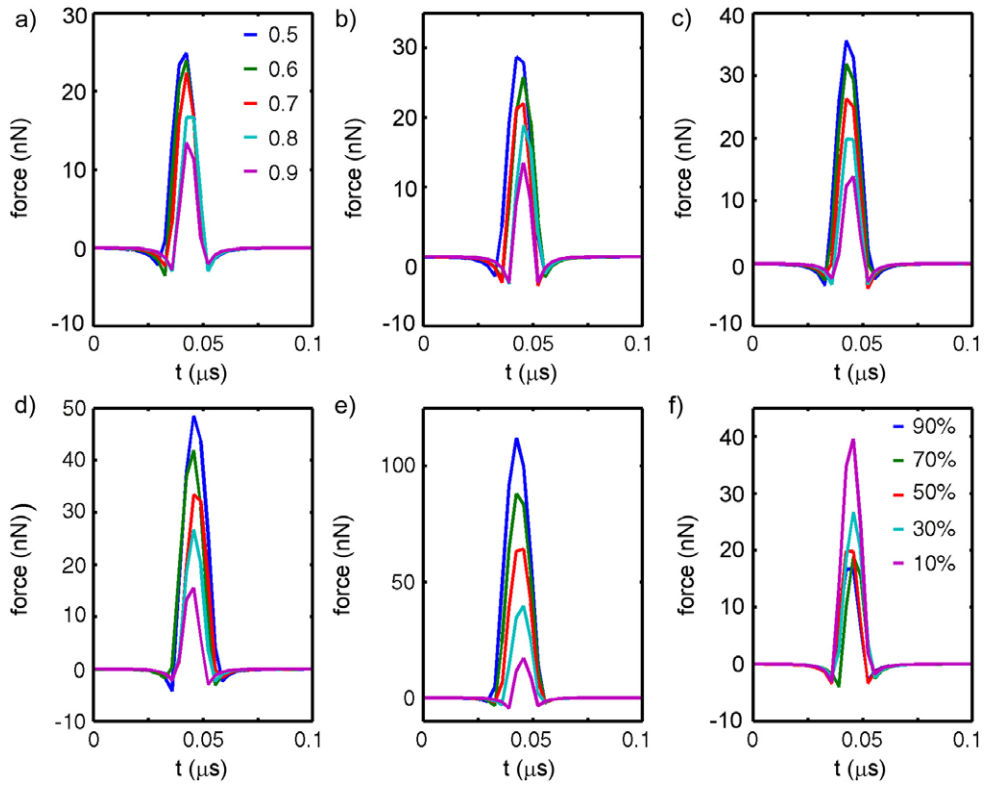

Figure 3. Simulated time-varying tip–sample forces for tapping operation on a 60 GPa surface (similar to mica). With drive frequency set at (a) 90%, (b) 70%, (c) 50%, (d) 30%, or (e) 10% below resonance, the maximum tapping force, total tapping force, and contact time increased with a reduction of set point ratio from 0.9 to 0.5. The legend in (a) applies to (a)–(e). (f) Time-varying tip–sample force interactions are compared at operating drive frequencies of different %'s below resonance at a set point ratio of 0.8. The maximum tapping force, total tapping force, and contact time increased as the cantilever was driven further below resonance.

2. Experimental details

2.1. Numeric simulations of tapping mode AFM

To investigate the relationship between imaging parameters and time-varying tapping forces, numerical simulations were performed with the aid of SIMULINK and MATLAB (MathWorks Inc., Natick, MA). Several key parameters in modeling cantilever dynamics are schematically shown in figure 1(a), while the complete SIMULINK model is shown in figure 1(b). In these simulations, the cantilever was modeled as a single degree of freedom damped driven harmonic oscillator [19–22].

$$m_{\text{eff}}\ddot{z} + b\dot{z} + k[z - D_0 + a_0 \sin(\omega t)] = F_{\text{ext}} \qquad (1)$$

where m_{eff} is the effective mass of a cantilever, b is the damping coefficient, k is the cantilever spring constant, a_0 is the drive amplitude, ω is the drive frequency, D_0 is the resting position of the cantilever base, F_{ext} is the tip–sample force, and z is the position of the cantilever with respect to the surface. The SIMULINK cantilever model is shown in figure 1(c).

During tapping mode operation, the cantilever oscillation results in a continual changing separation distance between the probe tip and sample surface, with the probe tip briefly contacting the surface during each oscillation cycle. This results in two tip–sample interaction regimes: (1) at large separation distance when the tip and surface are not in contact and (2) when the tip and surface are in contact during the tapping event. For large tip–sample separation distance, the external force can be approximated using the van der Waals interaction between a sphere and flat surface [23]:

$$F_{\text{ext}} = \frac{H R_{\text{tip}}}{6z^2} \qquad \text{for } z > a_{\text{DMT}} \qquad (2)$$

where H is the Hamaker constant, R_{tip} is the tip radius, and a_{DMT} is the interatomic distance parameter of a Derjaguin–Muller–Toporov (DMT) potential [24]. At the bottom of each oscillation cycle, the probe tip contacts the surface when the separation distance z is smaller than the interatomic distance (a_{DMT}). Under these conditions, the tip–sample force can be described by a DMT potential.

$$F_{\text{ext}} = \frac{4}{3\pi k_{\text{eff}}}\sqrt{R}(a_{\text{DMT}} - z)^{3/2} - \frac{H R_{\text{tip}}}{6a_{\text{DMT}^2}} \qquad \text{for } z \leqslant a_{\text{DMT}} \qquad (3)$$

with

$$k_{\text{eff}} = \frac{1 - \nu_{\text{tip}}^2}{\pi E_{\text{tip}}} + \frac{1 - \nu_{\text{sample}}^2}{\pi E_{\text{sample}}} \qquad (4)$$

where E_{tip}, ν_{tip} and E_{sample}, ν_{sample} are, respectively, the Young's modulus and Poisson coefficient of the tip and the sample. The tip/sample force model is shown in figure 1(d).

The model also contains a feedback loop equipped with a PID controller (although only the integral gain was used

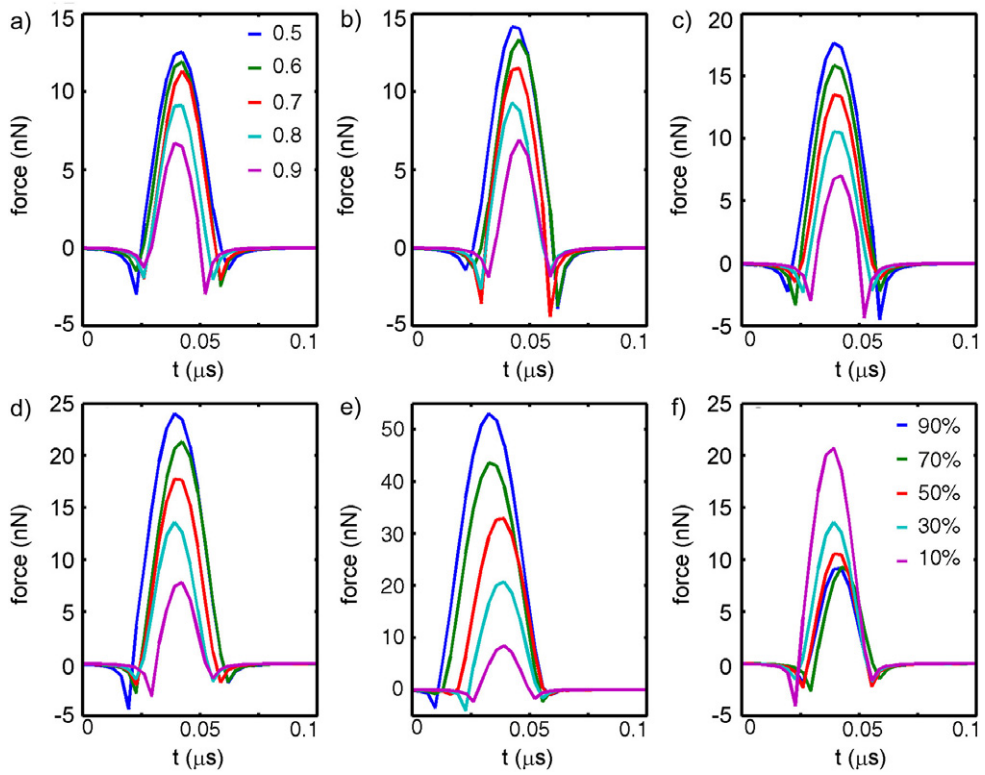

Figure 4. Simulated time-varying tip–sample forces for tapping operation on a 2 GPa surface (similar to polystyrene). With drive frequency set at (a) 90%, (b) 70%, (c) 50%, (d) 30%, or (e) 10% below resonance, the maximum tapping force, total tapping force, and contact time increased with a decreasing set point ratio. The legend in (a) applies to (a)–(e). For any given combination of set point and drive frequency, the total force was equal to the total force for the same parameters as measured on the 60 GPa surface (figure 3). (f) Time-varying tip–sample force interactions were compared at operating drive frequencies of different %'s below resonance at a set point ratio of 0.8. The maximum tapping force, total tapping force, and contact time increased as the cantilever was driven further below resonance.

in this study), which allows for a more complete simulation of the scanning process in tapping mode AFM [7]. The feedback loop was implemented by measuring the cantilever amplitude, comparing it to the specified set point, and adjusting the cantilever position to maintain the set point using an integral gain. The cantilever amplitude was measured by inspecting the cantilever position signal over the length of one oscillation cycle using signal processing tools available in SIMULINK. This feature allows for simulating the process of acquiring an AFM scan line in which a well-defined feature is contained by feeding predetermined surface topography information into the model. The effect of altered sample Young's modulus on the imaging process can also be explored by changing the inputs into equation (4) and feeding the result into equation (3) (as shown in figure 1(d)). These changes in Young's modulus can be synchronized with the predetermined surface topography to model the imaging process on a wide array of scenarios, for example imaging a soft particle on a hard surface.

For numerical simulations, five different oscillation frequencies were explored. These drive frequencies were determined by finding the frequency at which the free cantilever oscillation amplitude was 90%, 70%, 50%, 30%, and 10% of the free cantilever amplitude at resonance for any given drive amplitude (as shown in figure 2(a)). For simplicity, these frequencies will be referred to as '*x*% below resonance'. For comparison between operating frequencies, the drive amplitude was adjusted so that the same cantilever free amplitude was achieved at each frequency.

2.2. AFM experimental details

Actual tapping mode AFM experiments were performed with a NanoScope V MultiMode scanning probe microscope (Veeco, Santa Barbara, CA) equipped with HarmoniX capabilities. HarmoniX microscopy operates simultaneously with tapping mode, allowing for the reconstruction of tip–sample force interactions by measuring the torsional amplitude at higher harmonic frequencies of the tapping mode drive frequency [12–16]. HarmoniX microscopy requires the use of specially designed probes where the tip is offset to one side of the cantilever. Imaging was performed with HarmoniX probe silicon cantilevers (Veeco, Santa Barbara, CA) with a nominal spring constant of $\sim$4 N m^{-1}, vertical resonance frequency of $\sim$60 kHz. During imaging, individual time-varying tip sample force interactions were captured using the NanoScope V's built in high speed data acquisition capabilities. Similar to simulations, operating frequencies were chosen to be 90%, 70%, 50%, 30%, and 10% below resonance (figure 2(b)). For each frequency, the drive amplitude was chosen to result in a free cantilever oscillation amplitude of 40 nm. For all

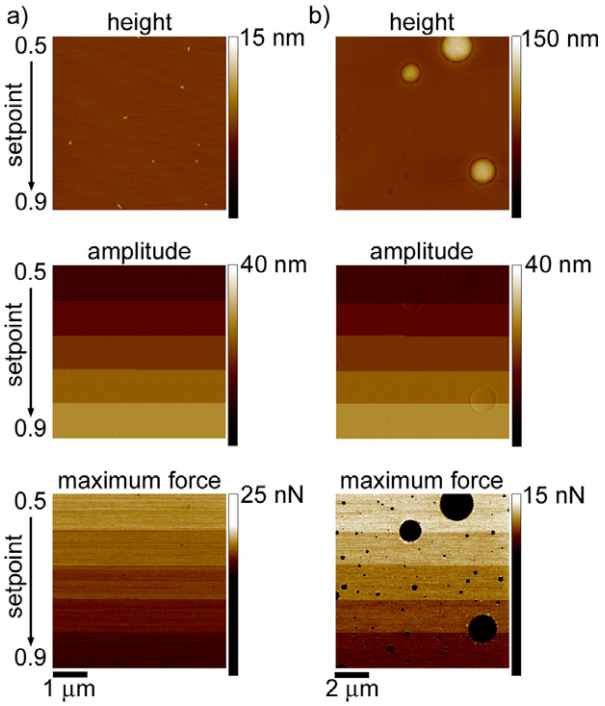

Figure 5. Tapping mode AFM images of (a) mica and (b) PS/EDPM taken with the HarmoniX capabilities. While imaging these two surfaces, the set point ratio was systematically changed at precise intervals. By forcing the capture of these images, data directly comparing the peak tapping force at any given operating frequency at a variety of set point ratios was obtained. A polynomial flattening procedure was applied to the height images (top images). As the same cantilever and imaging parameters were used to image both surfaces, the measured amplitudes at any given set point ratio were the same on both surfaces (middle images). While the resulting maximum (peak) forces measured on each surface decreased as the set point ratio goes to 1, the maximum force for any given set point was larger on the harder mica surface (bottom images).

experiments comparing set point and drive frequency, the gains and scan rate remained constant.

Tapping mode AFM HarmoniX experiments were performed on a variety of surfaces: mica (Ted Pella Inc, Redding, CA), Polystyrene/ethylene propylene diene M-class rubber mixture (HarmoniX standardization sample provided by Veeco, Santa Barbara, CA), and melted polystyrene beads on silicon. A sparse number of small protein aggregates (∼3 nm tall) were deposited on the mica to provide small features that could be used to verify that the probe trip was properly tracking the mica surface during imaging. Preparation of the melted polystyrene bead sample was prepared by sparsely depositing 200 nm polystyrene beads on a freshly cleaned silicon substrate. These substrates were then heated to 250 °C for 1–2 h, followed by plasma treatment. This process was repeated until PS features of the appropriate size were observed in AFM images.

3. Results and discussion

In an effort to understand the effect set point and operating frequency have on the time-varying tip–sample force associated with tapping mode AFM, single degree of freedom simulations were performed with parameters based on the typical properties of commercially available HarmoniX cantilevers. These typical parameters were as follows: resonance frequency of 60 kHz, spring constant of 4 N m^{-1}, and free amplitude of 40 nm. As tapping mode AFM is commonly used to image a variety of surfaces, we performed simulations of tapping mode AFM on two model surfaces of different Young's moduli, a 60 GPa surface (model of mica) and a 2 GPa surface (model of polystyrene). While these simulations could have been performed in the steady state, we chose to use a feedback loop to actively maintain the tapping amplitude.

Simulations were performed at a series of set points at several operating frequencies below resonance. Individual time-varying tip–sample force interactions obtained from numerical simulations are shown for the 60 and 2 GPa model surfaces in figures 3 and 4 respectively. The maximum force and total tip/sample force per oscillation cycle were investigated. The maximum force is defined as the peak or largest force experienced between the tip and sample. The total force is defined as the sum of the entire tip/sample force interaction over one cantilever oscillation cycle or the force integrated over one cycle. On both surfaces, the tapping force (both maximum and total force per oscillation) systematically decreased as the set point ratio was changed from 0.5 to 0.9. This relationship between set point and tapping force was independent of operating frequency. That is, at any given operating frequency, the associated tapping forces were smaller as the set point ratio approached 1. However, the increase in tapping force associated with reducing the set point ratio was larger when operating further below resonance. While the total force between the tip and surface per oscillation cycle remained constant for any given set point ratio (total force on 60 GPa surface was the same as on the 2 GPa surface), closer inspection of these simulated force profiles revealed that for any given combination of set point ratio and operating frequency that the maximum (or peak) tapping force was higher on the 60 GPa surface in comparison to the softer 2 GPa surface with a corresponding longer contact time for the softer surface. On both surfaces, the tapping forces (total and maximum) were larger at any given set point ratio as the cantilever was driven further below resonance, as is demonstrated in figures 3(f) and 4(f) for a set point of 0.8.

To verify the relationship between set point ratio and tip–sample forces, we imaged two distinct surfaces, mica and polystyrene/ethylene propylene diene M-class rubber mixture (PS/EPDM), using the HarmoniX imaging mode, which allows for the direct measurement of the time-varying tip–sample forces during imaging. Small protein aggregates were sparsely deposited on the mica surface (∼0.5 aggregate per square micron) to ensure that chosen operating parameters were able to track the surface. The PS/EPDM sample was predominantly PS, providing ample room to measure the tapping forces on PS with the EPDM features providing evidence that the surfaces was being adequately tracked. These surfaces were chosen due to their respective Young's moduli near those of the model surfaces used in simulation, providing relatively hard and soft

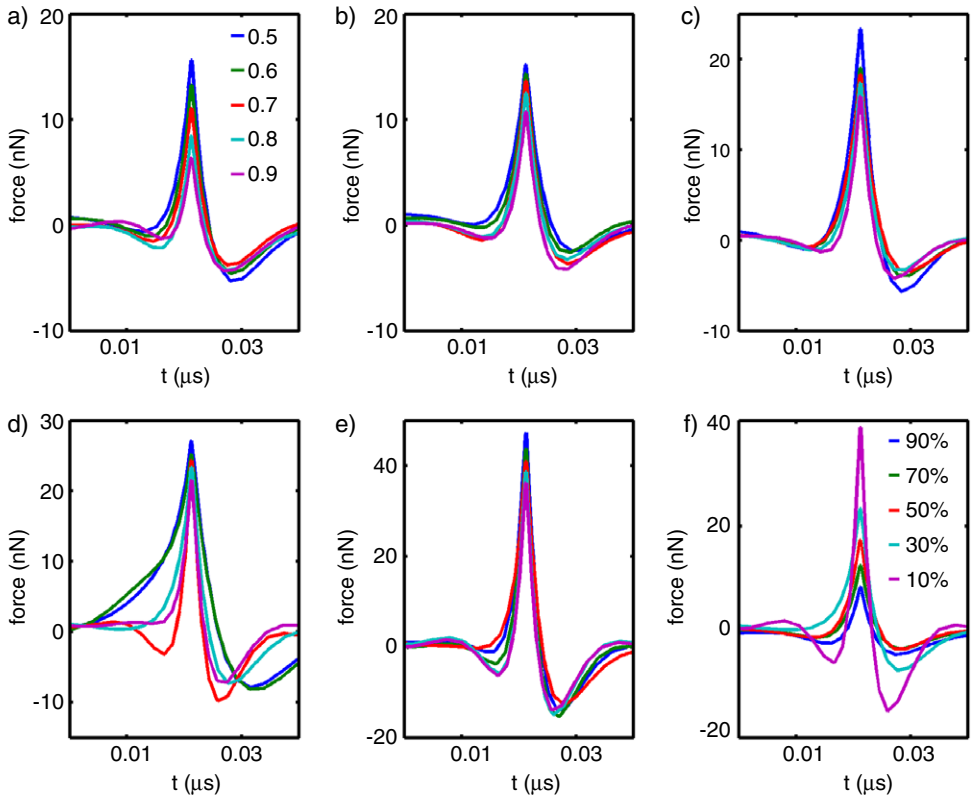

Figure 6. Time-varying tip–sample forces interactions measured in real experiments on mica. With drive frequency set at (a) 90%, (b) 70%, (c) 50%, (d) 30%, or (e) 10% below resonance, the maximum tapping force, total tapping force, and contact time increased with a decrease in set point ratio as predicted by simulation. The legend in (a) applies to ((a)–(e)). (f) Time-varying tip–sample force interactions are compared at operating drive frequencies of different %'s below resonance at a set point ratio of 0.8. As was predicted by simulation, the maximum tapping force, total tapping force, and contact time increased as the cantilever was driven further below resonance.

surfaces for experimentation, while still being within the range in which HarmoniX can accurately measure modulus [14]. While imaging these two surfaces, we systematically changed the set point ratio at precise intervals. By forcing the capture of these images, we were able to obtain images of these surfaces that directly compared the maximum (peak) tapping force at any given operating frequency at a variety of set point ratios.

Figure 5 shows representative images from this experiment for a cantilever operated at 70% below resonance. Topography images of the mica and PS/EPDM sample displayed no apparent changes as the set point ratio approaches 1. However, this was primarily due to the application of a polynomial line flattening procedure to the image to correct for image curvature. The impact of set point on measured height profiles will be more precisely explored by simulation and experiment on a soft step presented later. The amplitude images of both surfaces displayed a distinct pattern due to the change in set point during imaging. While the drive amplitude was chosen to obtain a free cantilever amplitude of 40 nm, the amplitude image corresponds to tapping amplitudes of 20 nm (top of the image, set point ratio of 0.5), 24 nm (set point ratio of 0.6), 28 nm (set point ratio of 0.7), 32 nm (set point ratio of 0.8), and 36 nm (bottom of image, set point ratio of 0.9). As the same cantilever, driven at the same frequency and drive amplitude, was used to image both surfaces, the amplitude values obtained on the two surfaces are identical for any given set point ratio. The maximum tapping force images show a corresponding decrease in the magnitude of this peak force, as would be predicted from our simulation, as the set point was systematically changed from 0.5 to 0.9. While the tapping amplitude obtained on the two different surfaces are clearly the same due to the precise control of the set point ratio, the resulting maximum tapping force was higher on the harder mica surface for any given set point in comparison to the corresponding maximum tapping force on the polystyrene portions of the softer sample (compare the scale bars for each image). This difference in maximum tapping force was predicted by our simulations.

To more systematically compare the time-varying tapping forces in real experiments, we used the high speed data capture capabilities of the HarmoniX mode to capture individual force profiles on the mica and PS/EDPM surfaces. These force profiles were captured at a series of set point ratios at several operating frequencies below resonance and are presented in figures 6 and 7 for mica and PS/EDPM respectively. As was seen in the maximum tapping force images (figure 5), the maximum tapping force systematically decreased as the set point ratio is changed from 0.5 to 0.9 on both surfaces at all operating frequencies. Closer inspection of these force profiles reveal that, as predicted in simulation, for any given condition the maximum tapping force was higher on mica in comparison to PS, with a corresponding longer contact time on the softer PS surface. However, the total force per oscillation cycle,

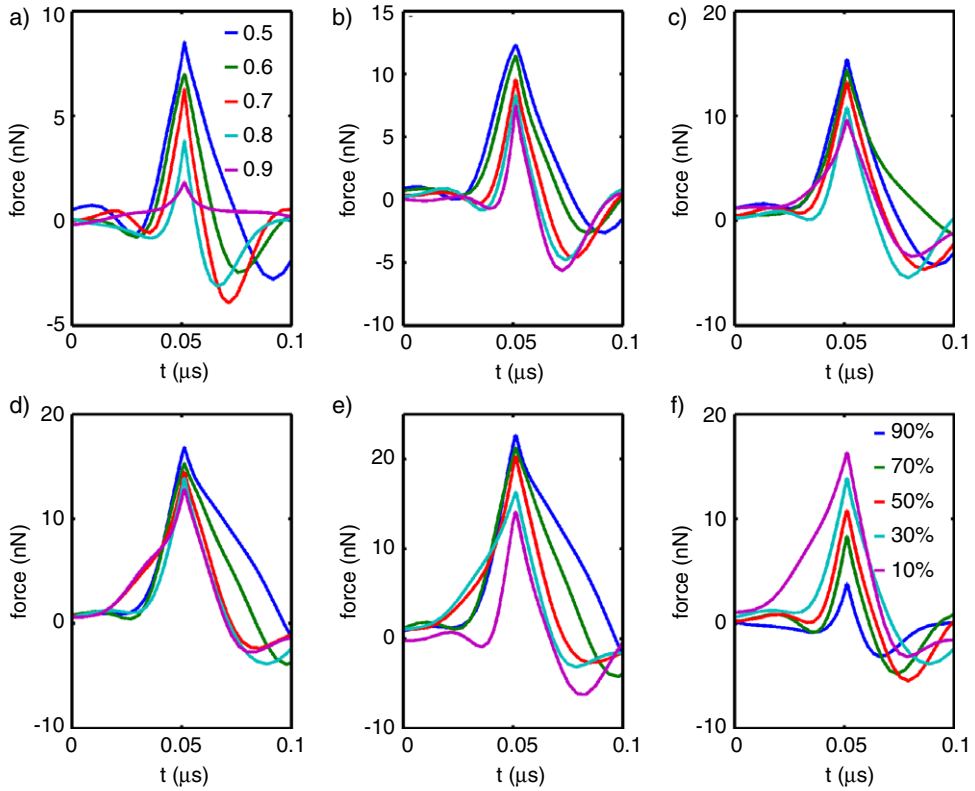

Figure 7. Time-varying tip–sample forces interactions measured in real experiments on polystyrene. With drive frequency set at (a) 90%, (b) 70%, (c) 50%, (d) 30%, or (e) 10% below resonance, the maximum tapping force, total tapping force, and contact time increased with a decrease in set point ratio as predicted by simulation. The legend in (a) applies to (a)–(e). For any given combination of set point and drive frequency, the total force was equal to the total force for the same parameters as measured on the mica surface (figure 6). (f) Time-varying tip–sample force interactions are compared at operating drive frequencies of different %'s below resonance at a set point ratio of 0.8. As was predicted by simulation, the maximum tapping force, total tapping force, and contact time increased as the cantilever was driven further below resonance.

defined as the sum of the tip/sample force during the course of one oscillation cycle, remained relatively constant between the different surfaces for any combination of set point ratio and operating frequency. On both surfaces, the tapping forces were larger at any given set point as the cantilever is driven further below resonance, as is demonstrated in figures 6(d) and 7(d) for a set point of 0.8.

While we have established that total force and maximum force increased with smaller set point ratios and with operation further below resonance, we next wanted to determine the impact of these increased forces on the process of acquiring an image. Therefore, we performed a series of numerical simulations of imaging a soft 12 nm tall rectangular step (figure 8(a)). The Young's modulus was 100 GPa before and after the step on our model surface with a reduction to 2 GPa on the step. The simulation parameters were chosen to correspond to imaging a 1 μm line with a scan rate of 1 Hz. Free oscillation amplitude of the cantilever was 40 nm. Simulations were performed with set point ratios of 0.9, 0.8, 0.7, 0.6, and 0.5 for operating frequencies 90%, 70%, 50%, 30%, and 10% below resonance. For these simulations, we only employed the integral gain in our feedback loop, and the value of the gain remained constant under all conditions. The AFM model was able to track the surface step under all simulation conditions; however, the height of the trace over the step was consistently smaller than the actual step height. This reduced measured step height was caused by the different compressibility, or softness, of the step in comparison to its more rigid surroundings. This phenomenon is the basis of compliance-based contrast in tapping mode AFM. Due to the implementation of the feedback loop which maintains constant cantilever amplitude during scanning (with the exception of edges, where transients appeared while the feedback loop was trying to restore the cantilever tapping amplitude to the set point), the total force in each oscillation cycle remained constant while the peak tapping force decreased on the softer step accompanied by an increase in contact time. For any given operating frequency, the compression of the soft step increased as the set point ratio was lowered, due to the higher tapping forces associated with lower set point ratios. As the tapping forces increased at a faster rate as a function of lowering the set point ratio when the cantilever is driven further below resonance, the compression of the soft step due to a reduction in set point ratio was more pronounced at operating frequencies further below resonance. As the magnitude of tapping force is also correlated with operating frequency, sample compression increased when operating further below resonance at any given set point ratio (figure 8(g)).

We next verified our simulation results in a real experimental system. For these experiments, we imaged the

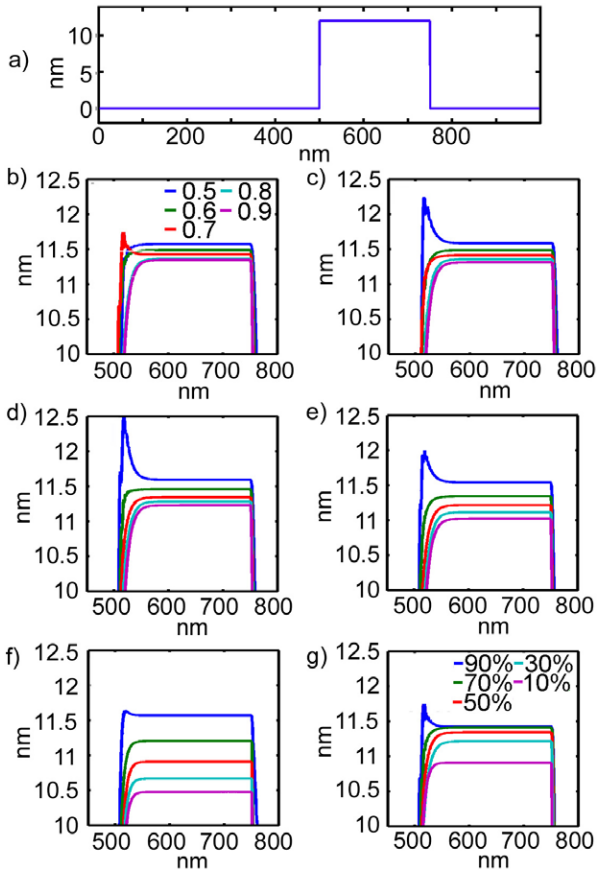

Figure 8. Tapping mode AFM simulations of imaging a soft step on a hard surface under various operating conditions. (a) The model topography used in the simulations is represented. The Young's modulus before and after the step was 100 GPa and 2 GPa on the step. Simulations of imaging this model topography were performed with various set point ratios ranging from 0.5 to 0.9 and at different operating frequencies below resonance. The integral gain was kept constant for all simulations. A series of simulated scan lines taken over the soft feature are shown as a function of set point ratio for operating frequencies (b) 90%, (c) 70%, (d) 50%, (e) 30%, and (f) 10% below resonance. The legend in (b) applies to (b)–(f). At all frequencies below resonance, the measured height of the step decreased as a function of smaller set point ratios due to compression of the soft feature. (g) The compression of the soft step at operating drive frequencies of different %'s below resonance at a set point ratio of 0.7 is compared. Compression increased as the system was operated further below resonance.

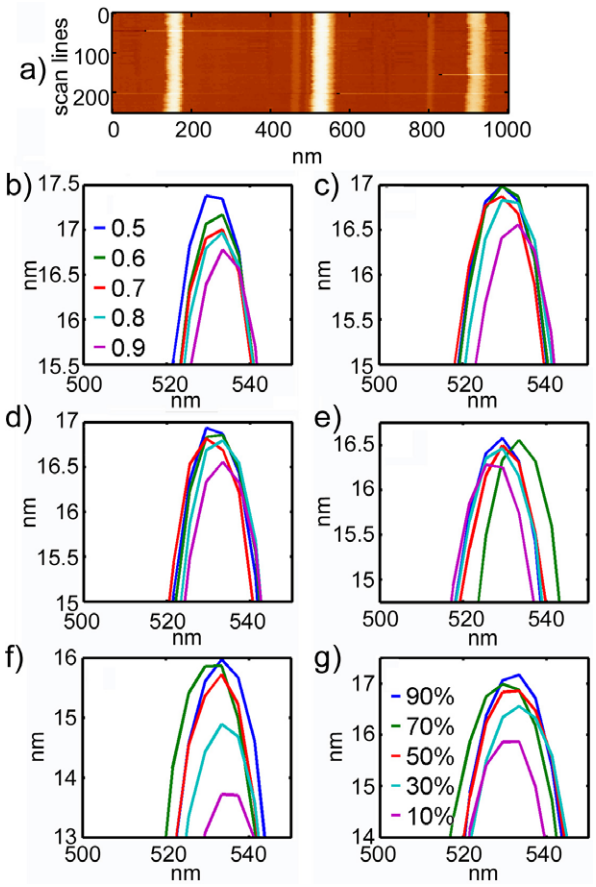

Figure 9. Experimental verification of sample compression due to increased tapping forces associated with changes in set point ratio and drive frequency. (a) A representative tapping mode AFM images used in this experiment in which a polystyrene features was imaged with the slow scan axis disabled. The feature was imaged with set point ratios ranging from 0.5 to 0.9 and at different operating frequencies ranging from 10% to 90% below resonance. A series of scan lines taken over the feature at approximately 530 nm in the image shown in (a) are represented as a function of set point ratio for operating frequencies (b) 90%, (c) 70%, (d) 50%, (e) 30%, and (f) 10% below resonance. The legend in (b) applies to (b)–(f). At all frequencies below resonance, the measured height of the polystyrene feature decreased as a function of smaller set point ratios due to compression. (g) The compression of the polystyrene feature at operating drive frequencies of different %'s below resonance at a set point ratio of 0.6 are compared. As was predicted by simulation, compression increased as a function of % below resonance.

same line (slow scan axis disabled) over a small polystyrene feature deposited on silicon with different set point ratios and operating frequencies (figure 9(a)). Again, we systematically changed the set point ratio at precise intervals. By forcing the capture of these images, we were able to obtain a series of line scans of the same feature at any given operating frequency at a variety of set points. Each profile presented is an average of 10 scan lines (figures 9(b)–(g)). For any given operating frequency, the measured height of the PS feature was smaller as the set point ratio was changed from 0.9 to 0.5, indicating a higher degree of compression. As was observed with the model, compression appeared to be more sensitive to set point ratio as the cantilever is driven further below resonance. As would be expected for any given set point ratio, the compression was larger when operated further below resonance, as shown for set point ratio 0.6 in figure 9(g).

As the tip–sample forces associated with imaging under all operating conditions compressed the soft step in simulation and the PS in real AFM experiments, we next determined if there was a simple relationship between the maximum tip–sample force and observed feature height (figure 10). For simulations presented in figure 8, observed feature height had a linear relationship with the maximum tip–sample force at all operating frequencies (table 1), with the intercepts (11.7–11.9 nm) of the best fit line approaching the known true height of the feature step (12 nm). This linear relationship appeared independent of operating frequency, as the simulated data taken

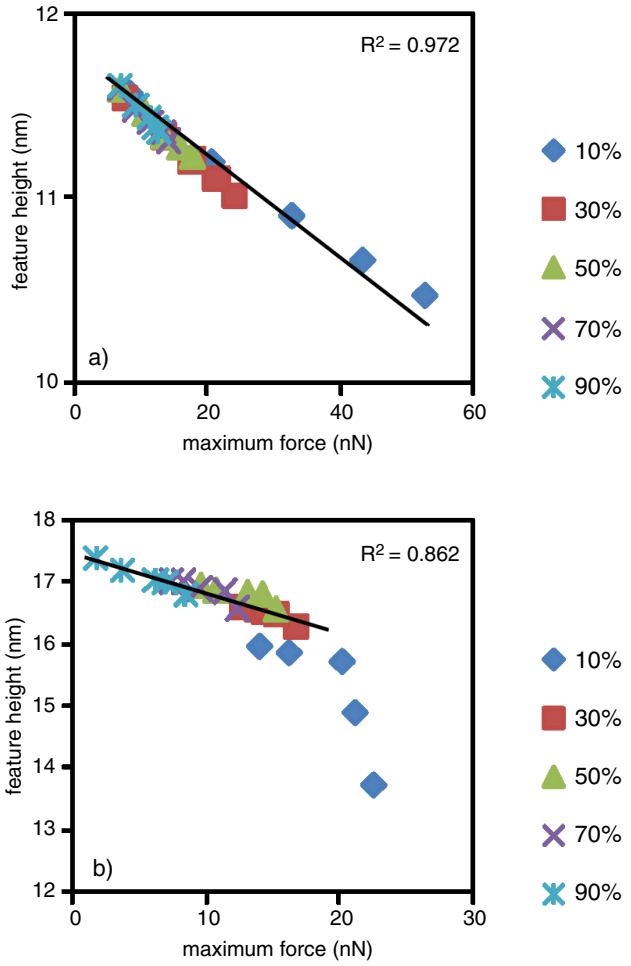

Figure 10. Measured feature height of a soft step as a function of maximum tapping force for (a) simulations and (b) real experiments. (a) A linear relationship between the measured feature height and maximum tapping force was observed in simulations (figure 8) at all operating frequencies. The R^2 value corresponds to the best fit line for all data points (simulations at all operating frequencies and set point ratios). (a) A linear relationship was also observed between the measured feature height and maximum tapping force in real tapping mode AFM experiments (figure 9) except at high maximum tip–sample forces (>20 nN). The R^2 value corresponds to the best fit line for all data points excluding those when the operating frequency was 10% below resonance due to the associated large maximum tapping forces.

(This figure is in colour only in the electronic version)

as a whole under all conditions remained linear. The linear relationship between measured feature height and maximum tip–sample force was also present in real tapping mode AFM experiments when operated at 90%, 70%, 50%, and 30% below resonance (table 1). However at 10% below resonance (which is associated with higher imaging forces), the linear relationship no longer held. Analysis of the experimental data, excluding that taken at operating frequency 10%, the estimated height of the PS feature was ∼17.4 nm. Taken collectively, this analysis suggests that collecting images at varying tip–sample forces can allow for the estimation of true heights of compressible surface features, provided that the imaging forces are not excessively large.

Table 1. Comparison of intercept and R^2 values for best fit lines of observed feature height versus maximum tip–sample tapping force of both simulated and experimental data.

Simulation			Experiment		
x% below resonance	Intercept (nm)	R^2	x% below resonance	Intercept (nm)	R^2
90	11.9	0.99	90	17.5	0.98
70	11.8	0.98	70	17.6	0.86
50	11.8	0.99	50	17.4	0.84
30	11.8	0.99	30	17.6	0.92
10	11.7	0.99	10	19.3	0.65
All	11.7	0.97	All except 10%	17.4	0.86

4. Conclusions

As tapping mode AFM has become a ubiquitous technique for obtaining topography images of surfaces and measuring material properties at the nanoscale, a deeper understanding of the interaction between the probe tip and surface has become increasingly important. In order to improve the operation of tapping mode AFM, reduce the obtrusiveness of the imaging process, obtain quantitative explanations of measured material properties, and develop new techniques to measure different mechanical properties, the relationship between tip–surface interactions and the dynamics of the oscillating cantilever need to be resolved. While numeric simulation have long been used to understand the tip–sample force interactions associated with tapping mode AFM [2–10], many of the valuable insights obtained in such studies have not been experimentally verified due to the inability to obtain time-varying tip–sample force interactions while operating AFM in the tapping mode. With the advent of new techniques [11–16], verification of these insights provided by numeric simulations is now achievable. The presented results verify that numerical simulations of tapping mode AFM based on a simple single degree of freedom point mass model capture many of the salient features associated with time-varying tip–sample forces as well as the impact of these forces on the imaging process. As analytical and numerical models are used extensively in understanding AFM imaging and in developing methods to evaluate material properties, it is imperative that AFM models are experimentally verified.

Acknowledgments

This work was supported by West Virginia University (start-up package). The author acknowledges Dr Lloyd Carroll for supplying the polystyrene beads and for assistance in preparing these samples.

References

[1] Binnig G, Quate C F and Gerber C 1986 Atomic force microscope *Phys. Rev. Lett.* **56** 930–3
[2] Garcia R and Perez R 2002 Dynamic atomic force microscopy methods *Surf. Sci. Rep.* **47** 197–301

[3] Paulo A S and Garcia R 2002 Unifying theory of tapping-mode atomic-force microscopy *Phys. Rev.* B **66** 041406
[4] Rodriguez T R and Garcia R 2002 Tip motion in amplitude modulation (tapping-mode) atomic-force microscopy: comparison between continuous and point-mass models *Appl. Phys. Lett.* **80** 1646–8
[5] Hashemi N, Dankowicz H and Paul M R 2008 The nonlinear dynamics of tapping mode atomic force microscopy with capillary force interactions *J. Appl. Phys.* **103** 093512
[6] Legleiter J and Kowalewski T 2005 Numerical simulations provide insights into fluid tapping-mode atomic force microscopy *Appl. Phys. Lett.* **87** 163120
[7] Kowalewski T and Legleiter J 2006 Imaging stability and average tip–sample force in tapping mode atomic force microscopy *J. Appl. Phys.* **99** 064903
[8] Zitzler L, Herminghaus S and Mugele F 2002 Capillary forces in tapping mode atomic force microscopy *Phys. Rev.* B **66** 155436
[9] Raman A, Melcher J and Tung R 2008 Cantilever dynamics in atomic force microscopy *Nano Today* **3** 20–27
[10] Varol A, Gunev I, Orun B and Basdogan C 2008 Numerical simulation of nano scanning in intermittent-contact mode AFM under Q control *Nanotechnology* **19** 075503
[11] Legleiter J, Park M, Cusick B and Kowalewski T 2006 Scanning probe acceleration microscopy (SPAM) in fluids: mapping mechanical properties of surfaces at the nanoscale *Proc. Natl Acad. Sci USA* **103** 4813–8
[12] Sahin O 2008 Accessing time-varying forces on the vibrating tip of the dynamic atomic force microscope to map material composition *Isr. J. Chem.* **48** 55–63
[13] Sahin O 2008 Time-varying tip–sample force measurements and steady-state dynamics in tapping-mode atomic force microscopy *Phys. Rev.* B **77** 115405
[14] Sahin O and Erina N 2008 High-resolution and large dynamic range nanomechanical mapping in tapping-mode atomic force microscopy *Nanotechnology* **19** 445717
[15] Sahin O 2007 Harnessing bifurcations in tapping-mode atomic force microscopy to calibrate time-varying tip–sample force measurements *Rev. Sci. Instrum.* **78** 103707
[16] Sahin O, Magonov S, Su C, Quate C F and Solgaard O 2007 An atomic force microscope tip designed to measure time-varying nanomechanical forces *Nat. Nanotechnol.* **2** 507–14
[17] Stark M, Stark R W, Heckl W M and Guckenberger R 2002 Inverting dynamic force microscopy: from signals to time-resolved interaction forces *Proc. Natl Acad. Sci USA* **99** 8473–8
[18] Xu X, Carrasco C, de Pablo P J, Gomez-Herrero J and Raman A 2008 Unmasking imaging forces on soft biological samples in liquids when using dynamic atomic force microscopy: a case study on viral capsids *Biophys. J.* **95** 2520–8
[19] Kuhle A, Sorensen A H and Bohr J 1997 Role of attractive forces in tapping tip force microscopy *J. Appl. Phys.* **81** 6562–9
[20] Salapaka M V, Chen D J and Cleveland J P 2000 Linearity of amplitude and phase in tapping-mode atomic force microscopy *Phys. Rev.* B **61** 1106
[21] Burnham N A, Behrend O P, Oulevey F, Gremaud G, Gallo P, Gourdon D, Dupas E, Kulik A J, Pollock H M and Briggs G A D 1997 How does a tip tap? *Nanotechnology* **8** 67–75
[22] Song Y X and Bhushan B 2008 Atomic force microscopy dynamic modes: modeling and applications *J. Phys.: Condens. Matter* **20** 225012
[23] Israelachvili J 1992 Van der Waals forces between surfaces *Intermolecular and Surface Forces* (London: Academic) pp 176–212
[24] Derjaguin B V, Muller V M and Toporov Y P 1975 Effect of contact deformations on the adhesion of particles *J. Colloid Interface Sci.* **53** 314–26